Clinical Characterization, Natural History, and Detailed Phenotyping of *NMNAT1*-Associated Leber Congenital Amaurosis

YOO JIN LEE, HYUN CHUL JEONG, JEONG HUN KIM, AND DONG HYUN JO

• PURPOSE: To characterize the clinical phenotype and disease progression in patients with *NMNAT1*-associated Leber congenital amaurosis (LCA) within the Korean population.
• DESIGN: Retrospective, observational case series.
• SUBJECTS: Fourteen patients with LCA with biallelic variants of *NMNAT1* at a single tertiary referral center.
• METHODS: Electronic medical records were reviewed for medical history, ophthalmic examinations, and molecular diagnoses, both cross-sectionally and longitudinally.
• MAIN OUTCOME MEASURES: Ophthalmic examination findings were evaluated and retinal phenotypic characteristics were assessed using multimodal imaging.
• RESULTS: All patients exhibited early-onset, rapidly progressive bilateral retinal degeneration with pronounced central involvement. The condition was characterized by multiple atrophic lesions that coalesced into a large central retinal scar by age 2. The condition stabilized around 4 years of age. Fluorescein angiography demonstrated central hypofluorescence with visible choroidal vasculature. Optical coherence tomography showed significant retinal thinning, outer retinal layer disruption, and retinal pigment epithelial atrophy. Most patients maintained light perception vision or better, with minimal deterioration of visual acuity after the age of 2. All patients were hyperopic and exhibited undetectable electroretinography and visual-evoked potential responses.
• CONCLUSIONS: *NMNAT1*-associated LCA is characterized by severe, early-onset retinal degeneration with rapid progression, followed by stabilization. This distinct temporal pattern of disease progression suggests a potential therapeutic window in early childhood, emphasizing the importance of early diagnosis and regular monitoring for potential interventions. (Am J Ophthalmol 2025;271: 396–406. © 2024 Elsevier Inc. All rights are reserved, including those for text and data mining, AI training, and similar technologies.)

Accepted for publication December 16, 2024.

From the Department of Medicine (Y.J.L.), Seoul National University College of Medicine, Seoul, Republic of Korea; Department of Biomedical Sciences (H.C.J., J.H.K.), Seoul National University College of Medicine, Jongno-gu, Seoul, Republic of Korea; Department of Ophthalmology (J.H.K.), Seoul National University College of Medicine, Jongno-gu, Seoul, Republic of Korea; Department of Anatomy and Cell Biology (D.H.J.), Seoul National University College of Medicine, Jongno-gu, Seoul, Republic of Korea

Abbreviations: ERG, electroretinography; F&F, fixation and following; FA, fluorescein angiography; FAF, fundus autofluorescence; GVF, Goldmann visual field; HM, hand motion; IRB, Institutional Review Board; LCA, Leber congenital amaurosis; LP, light perception; MAF, minor allele frequency; NAD+, nicotinamide adenine dinucleotide; NLP, no light perception; *NMNAT1*, nicotinamide nucleotide adenylyltransferase 1; OCT, optical coherence tomography; ONL, outer nuclear layer; RPE, retinal pigment epithelium; USG, ultrasonography; VA, visual acuity; VEP, visual-evoked potential.

Inquiries to Dong Hyun Jo, Department of Anatomy and Cell Biology, Seoul National University College of Medicine, 103 Daehak-ro, Jongno-gu, Seoul, 03080, Republic of Korea; e-mail: lawrenc2@snu.ac.kr

INTRODUCTION

Leber congenital amaurosis (LCA; OMIM #204000) is the most severe form of inherited retinal dystrophy, typically presenting within the first year of life. With a worldwide prevalence of 1 in 30,000 to 81,000, LCA accounts for approximately 5% of all retinal dystrophies and affects 20% of visually impaired children attending special schools.[1-4] LCA is characterized by severely reduced visual function from birth, nystagmus, poor pupillary response, oculodigital sign, and non-recordable electroretinography (ERG).[5] Most LCA cases follow an autosomal recessive inheritance pattern, though some autosomal dominant forms have been identified.[5] To date, variants in more than 20 genes are known to cause LCA.[6,7]

Biallelic variants in the nicotinamide nucleotide adenylyltransferase 1 (*NMNAT1*; OMIM *608700) gene have been reported to cause LCA.[8] *NMNAT1* variants account for 4.9% to 18% of LCA cases, with a notably higher prevalence in East Asian and Australian populations, particularly in South Korea.[9-12] The c.709C>T (p.Arg237Cys) variant is particularly common, with all patients in a South Korean cohort carrying this variant.[10] This unique genetic pattern offers an opportunity to gain insights into the pathogenesis and progression of LCA within specific populations.

The *NMNAT1* gene, located on chromosome 1p36.22, encodes an essential enzyme involved in nicotinamide adenine dinucleotide (NAD+) biosynthesis.[13] Although *NMNAT1* is ubiquitously expressed and plays a crucial role in cellular metabolism and energy production, its variants pri-

0002-9394/$36.00
https://doi.org/10.1016/j.ajo.2024.12.016

marily cause retina-specific disease, highlighting the enzyme's importance in retinal health.[13,14] *NMNAT1* is particularly significant in the retina, where it is essential for both the development and maintenance of retinal photoreceptors.[15] This retina-specific pathology underscores the critical role of *NMNAT1* in retinal function, with variants in this gene consistently associated with early-onset, severe retinal degeneration.[16-18]

Previous studies have characterized the spatial distribution of retinal changes in *NMNAT1*-associated LCA, revealing a spectrum of severity.[8,12,16-22] The mildest cases, while still presenting as severe infantile blindness, show a cone-rod dystrophy phenotype with evidence of maldevelopment of the central retina.[23] However, there remains a need for comprehensive longitudinal data on the clinical course and phenotypic variability associated with specific *NMNAT1* variants, particularly the c.709C>T variant that is prevalent in certain populations.

Therefore, we conducted a thorough examination of patients harboring biallelic *NMNAT1* variants, including the c.709C>T variant, using both cross-sectional and longitudinal analyses. Understanding the specific phenotypic manifestations associated with this variant can lead to an earlier and more accurate diagnosis. Detailed descriptions of clinical phenotypes can inform the development of targeted therapies, including gene therapy approaches, which have shown promise in other forms of LCA, such as *RPE65*-associated LCA.[24] This comprehensive report of patients harboring *NMNAT1* variants provides insights into the clinical characteristics and outcomes associated with this prevalent variant, contributing to our understanding of genotype-phenotype correlations in *NMNAT1*-associated LCA.

METHODS

This was a single-center, retrospective, observational case series. This study was approved by the Institutional Review Board (IRB) of Seoul National University Hospital (IRB No. 2208-022-1346). This study adhered to the tenets of the Declaration of Helsinki. The ethics committee waived the requirement for informed consent due to the retrospective nature of the study.

• **PATIENT SELECTION:** Patients diagnosed with LCA, confirmed by molecular testing at Seoul National University Children's Hospital, Seoul, Republic of Korea, between January 2012 and October 2023, were included in this study. Among them, individuals carrying biallelic variants of the *NMNAT1* gene were included in the final analysis.

• **DATA COLLECTION:** A standardized review of the patients' electronic medical records was conducted to gather information on medical history, family history, and ophthalmic examinations. Ophthalmic examinations included visual acuity (VA) measurement, refractive error evaluation, fundus examination, fundus photography, fluorescein angiography (FA), fundus autofluorescence (FAF), optical coherence tomography (OCT), electroretinography (ERG), visual-evoked potential (VEP), Goldmann visual field (GVF) testing, and ultrasonography (USG).

Prior to all the examinations, the pupils were dilated. Fundus photographs were acquired using an Optos retinal imaging system (Optos, Marlborough, MA, USA) and a RetCam (Clarity Medical Systems, Inc., Pleasanton, CA, USA). The FA images were obtained using a RetCam (Clarity Medical Systems, Inc., Pleasanton, CA, USA). FAF data were acquired using an Optos retinal imaging system (Optos, Marlborough, MA, USA). The OCT data were obtained using a Heidelberg Spectralis OCT instrument (Heidelberg Engineering, Hemel Hempstead, UK). ERG and VEP measurements adhered to the International Society for Clinical Electrophysiology of Vision standards using commercially available systems (MonPack 1, Metrovision, Pérenchies, France; and Retiport32, Roland Consult, Brandenburg an der Havel, Germany).[25,26] Due to patient age and compliance considerations, an abbreviated protocol including scotopic (DA 3) and photopic (LA 3) ERG measurements was conducted. VEP measurements were obtained using monocular flash stimuli, with responses recorded from the right occipital lobe. Certified professionals conducted the GVF evaluations following established protocols. USG was performed using the Aviso V3.0.0 and ABSolu V1.0.4 systems (Quantel Medical, Cournon-d'Auvergne, France).

• **MOLECULAR DIAGNOSIS:** Genomic DNA was extracted from peripheral blood leukocytes using a commercial DNA extraction kit (QIAamp DNA Blood Maxi Kit; Qiagen, Hilden, Germany). Hybridization capture-based next-generation sequencing was performed to analyze a panel of 135 genes (including *AIPL1*, *CEP290*, *CRB1*, *CRX*, *GUCY2D*, *LCA5*, *NMNAT1*, *RDH12*, and *RPE65*) associated with LCA and related disorders. An Agilent SureSelectXT Custom enrichment kit (Agilent Technologies, Santa Clara, CA, USA) was used, targeting a genomic region of 0.5–2.9 Mb (version 170726_gr). NextGene software version 2.4.0.1 was used for the data analysis. GRCh37 (hg19) was used as the reference sequence.

• **VARIANT INTERPRETATION:** Variant interpretation adhered to the standards and guidelines established by the American College of Medical Genetics and Genomics (ACMG).[27] Variant nomenclature followed the guidelines set by the Human Genome Variation Society (HGVS). The ClinVar database (https://www.ncbi.nlm.nih.gov/clinvar/) was consulted to obtain additional information regarding variant pathogenicity. For variants with conflicting inter-

pretations or uncertain significance, pathogenicity was further assessed based on ACMG standards and guidelines.

RESULTS

• **DEMOGRAPHICS AND DISEASE ONSET:** Fourteen individuals from 12 families were included in this study (Table 1). Among these, 2 pairs of siblings were identified: Patients 7 and 8, and Patients 13 and 14. Eight patients were male (57%), and 6 were female (43%). All the patients were Korean. They did not report any consanguinity or family history of genetic eye diseases. All the patients were diagnosed with LCA, and the mean (± standard deviation, SD) age at diagnosis was 11.1 months (± 13.8 months). Among the 12 patients with available records of initial signs (excluding 2 patients whose signs could not be assessed), 9 patients (75%) presented with an inability to establish eye contact as the initial sign. The remaining 3 patients presented with esotropia, nystagmus, and poor response to light, respectively. The majority of patients presented signs before 6 months of age ($n = 10$), with all cases having signs identified by 1 year of age.

• **MOLECULAR DIAGNOSIS:** Genetic analysis revealed the presence of biallelic *NMNAT1* variants in all patients ($n = 14$). Specifically, 12 out of 14 patients harbored the c.709C>T (p.Arg237Cys) variant. For these 12 patients, the variants on the other allele were distributed as follows: 4 patients had the c.196C>T (p.Arg66Trp) variant, 4 had the c.116-2A>G variant, and the remaining 4 presented with c.56C>T (p.Pro19Leu), c.137G>T (p.Gly46Val), c.743T>C (p.Ile248Thr), and exon 2 deletion, respectively. The other 2 patients (Patient 13 and 14) carried *NMNAT1* c.736G>C (p.Glu246Gln) on 1 allele and *NMNAT1* exon 4–5 deletion on the other. The variants were classified according to ACMG guidelines as follows: the pathogenic variants included c.709C>T, c.196C>T, c.116-2A>G, exon 2 deletion, and exon 4–5 deletion; whereas the likely pathogenic variants included c.56C>T, c.137G>T, c.736G>C, and c.743T>C.

• **RETINAL PHENOTYPE AND DISEASE PROGRESSION:** We conducted a longitudinal study, observing a distinct pattern of bilateral retinal degeneration with prominent central involvement (Figure 1A–H). The mean (± SD) follow-up duration was 82.8 months (± 33.9 months) ($n = 12$, range: 15.8–136.4 months), allowing documentation of retinal changes at key developmental stages.

The condition was characterized by early onset, rapid progression, and an apparent slowing of visible deterioration. Within a few months after birth ($n = 9$, range: 2.4–6.4 months), multiple atrophic lesions emerged in a patchy geographic pattern with distinct borders (Figure 1A and B). Over the next 2 years, these lesions rapidly progressed and coalesced into a single, large macular scar by approximately 2 years of age (Figure 1C). Throughout this period, the central retinal atrophy demonstrated well-defined boundaries, while the overlapping parts changed into smooth borders. These lesions, resembling colobomas (pseudocolobomas), suggest loss of retinal tissue.

The degenerative process, characterized by progressive enlargement of atrophic lesions, typically reached its peak at approximately 4 years of age ($n = 7$, range: 41.8–64.2 months). Subsequent observations indicated a relative stabilization of the macular scar, characterized by a marked slowing in the visible progression of the lesion size. Beyond age 4, the lesion remained limited to the posterior pole, with minimal further expansion (Figure 1D).

Examination of the peripheral retina revealed degenerative changes in the retinal pigment epithelium (RPE) and scattered pigment clumping. Notably, patients with the c.196C>T variant on the second allele exhibited a more prominent degree of pigmentation than did patients with other variants (Figure 1I and J). In addition to the aforementioned clinical characteristics, patients exhibited retinal vessel attenuation and optic disc pallor (Figure 1).

• **FLUORESCEIN ANGIOGRAPHY AND FUNDUS AUTOFLUORESCENCE FINDINGS:** FA images demonstrated a well-demarcated area of central hypofluorescence, allowing clear visualization of the underlying choroidal vasculature within this region ($n = 6$; Figure 2A). Some patients exhibited additional hypofluorescent patches in the peripheral retina, suggesting blocking defects corresponding to the pigment deposits observed in color fundus photographs. The results also indicated a significant attenuation of the retinal vasculature.

Notably, 1 patient demonstrated intriguing FA progression. At 4.4 months, FA revealed hyperfluorescent patches within the hypofluorescent region (Figure 2B). The boundaries of the hyperfluorescent patches precisely delineated the margins of the atrophic regions observed in fundus photographs (Figure 1F). These hyperfluorescent patches manifested as well-demarcated areas with visible underlying choroidal vasculature, which remained consistent throughout the angiographic examination. Follow-up FA in this patient at 18.2 months revealed well-demarcated central hypofluorescence, similar to the findings in other patients (Figure 2C).

FAF imaging identified hypofluorescent areas in the posterior fundi ($n = 2$; Figure 2D). These areas of diminished FAF signals corresponded to the regions of RPE atrophy observed using other imaging modalities.

• **OCT ANALYSIS:** OCT imaging revealed characteristic retinal abnormalities ($n = 7$; Figure 2E and F). The most prominent feature was a staphyloma-like posterior bowing of the macula, indicating significant structural alterations. Within this area, marked disruption of retinal layer integrity was observed, particularly affecting the outer retinal layers.

TABLE 1. Clinical and Genetic Characteristics of Patients with *NMNAT1*-Associated LCA

ID	Sex	Variant 1		Variant 2		Age at diagnosis (months)	Age at exam (years)	VA	Refraction (OD/OS) (Dsph)	Initial presentation	Peripheral pigmentation	Oculo-digital sign	Cataract	Vitreous opacity	Nystagmus	Systemic
1	F	c.709C>T	p.Arg237Cys	c.196C>T	p.Arg66Trp	5.7	9	LP	+5.00/+5.00	Inability to establish eye contact	Prominent	+	+	+	+	
2	M	c.709C>T	p.Arg237Cys	c.196C>T	p.Arg66Trp	25.3	9	LP	+4.00/+4.50	Inability to establish eye contact	Prominent	+	-	+	+	DD
3	M	c.709C>T	p.Arg237Cys	c.196C>T	p.Arg66Trp	4.7	6	LP	+5.00/+6.00	Inability to establish eye contact	Prominent	+	+	+	+	
4	M	c.709C>T	p.Arg237Cys	c.196C>T	p.Arg66Trp	4.9	11	LP	+6.00/+5.50	Inability to establish eye contact	Prominent	+	+	-	+	
5	F	c.709C>T	p.Arg237Cys	c.116-2A>G	p.?	3.4	7	LP	+7.50/+8.50	Poor response to light	Minimal	+	-	-	+	
6	F	c.709C>T	p.Arg237Cys	c.116-2A>G	p.?	4.4	8	0.01	+1.00/+1.00	Esotropia	Minimal	+	+	+	+	
7	F	c.709C>T	p.Arg237Cys	c.116-2A>G	p.?	N/A	9	NLP	+9.50/+9.50	N/A	Minimal	N/A	+	+	N/A	
8	M	c.709C>T	p.Arg237Cys	c.116-2A>G	p.?	N/A	6	HM	+9.00/+9.00	N/A	Minimal	N/A	+	+	N/A	
9	M	c.709C>T	p.Arg237Cys	c.56C>T	p.Pro19Leu	2.4	3	Poor F&F	+3.50/+4.00	Inability to establish eye contact	Minimal	-	-	-	+	DD
10	M	c.709C>T	p.Arg237Cys	c.137G>T	p.Gly46Val	6.2	12	LP	+4.00/+4.00	Inability to establish eye contact	Minimal	+	+	+	+	DD, seizure, autism
11	M	c.709C>T	p.Arg237Cys	c.743T>C	p.Ile248Thr	4.0	4	LP	+4.50/+4.50	Inability to establish eye contact	Minimal	-	+	-	+	
12	F	c.709C>T	p.Arg237Cys	Exon 2 deletion		4.7	6	HM	+4.50/+4.50	Inability to establish eye contact	Prominent	-	-	+	+	
13	M	c.736G>C	p.Glu246Gln	Exon 4–5 deletion		48.9	9	FC 40 cm	+1.25/+1.25	Inability to establish eye contact	Minimal	-	+	-	+	
14	F	c.736G>C	p.Glu246Gln	Exon 4–5 deletion		18.9	12	FC 20 cm	+5.00/+5.00	Nystagmus	Minimal	-	-	-	+	

Patients 7 and 8, and Patients 13 and 14 are siblings. Age at exam refers to age at most recent examination. DD = developmental delay; F&F = fixation and following; FC = finger counting; HM = hand motion; LP = light perception; N/A = not available; NLP = no light perception; OD = right eye; OS = left eye; VA = visual acuity.

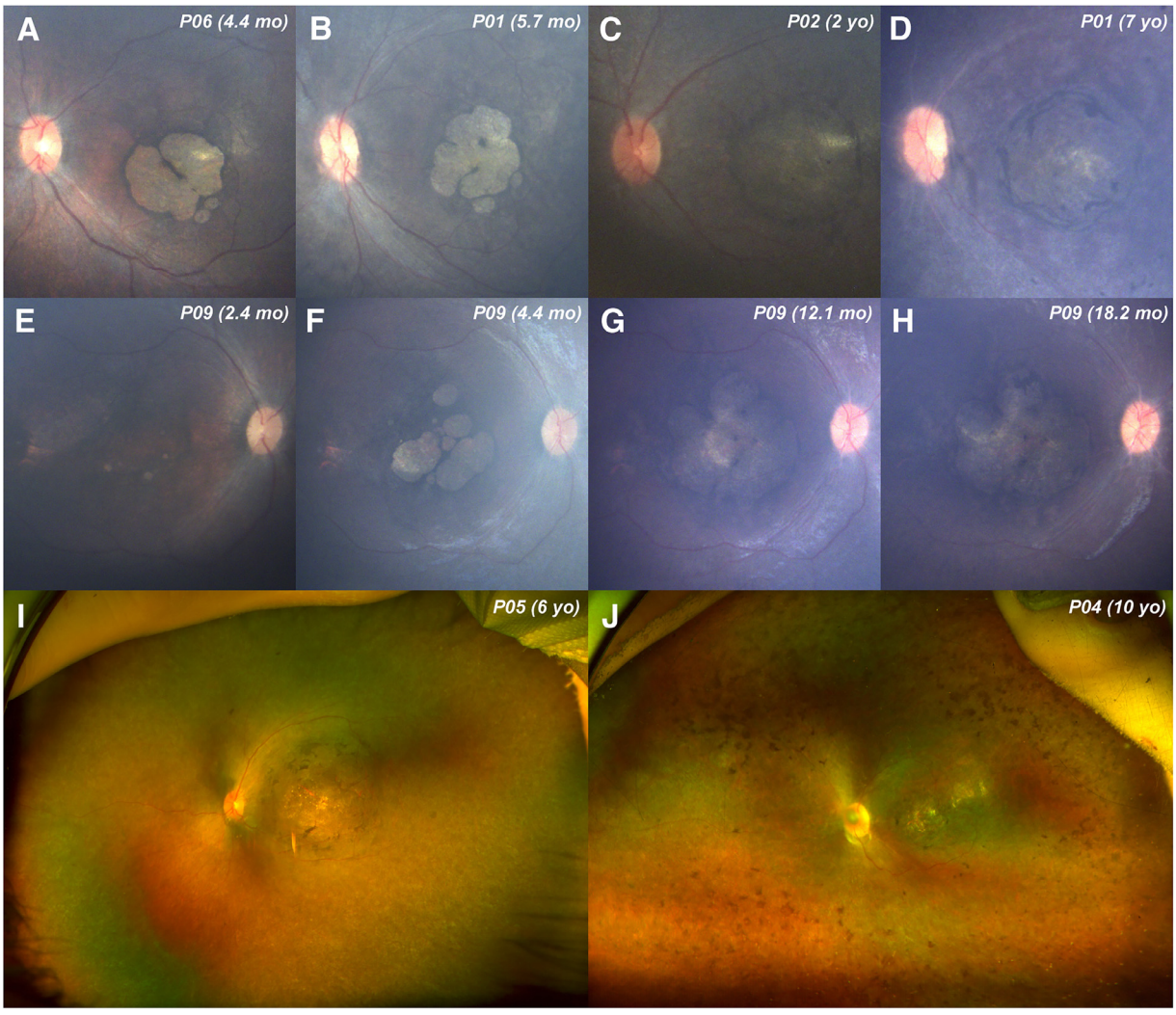

FIGURE 1. Retinal features of patients with *NMNAT1* variants. A, B, Fundus photographs of patients in the infantile period showing multiple patchy lesions in the central retina at 4.4 months (A) and 5.7 months (B). C, Single, large macular scar in a patient around 2 years of age (27.2 months). D, Stable fundus appearance, exhibiting nummular coloboma-like macular atrophy at 7 years of age. E–H, Fundus photographs of Patient 9 demonstrating progressive macular atrophy. E, Multiple atrophic scars at 2.4 months. F, Progression at 4.4 months. G, Coalescence of lesions with smooth borders at 12.1 months. H, Further enlargement at 18.2 months. I, A wide-field fundus photograph of a patient with the c.116-2A>G variant, showing minimal peripheral retinal pigmentation. J, A wide-field fundus photograph of a patient with the c.196C>T variant, demonstrating scattered peripheral retinal pigmentation.

The central region exhibited severe thinning of the outer nuclear layer (ONL), suggesting substantial loss of photoreceptor nuclei. The RPE layer showed significant attenuation and disruption, with areas of complete absence corresponding to regions of most severe outer retinal loss. This RPE atrophy was pronounced within the staphylomatous area but extended beyond its margins. Notably, despite the severe outer retinal and RPE changes, the inner retinal layers appeared relatively preserved. The choroid demonstrated thinning in some patients.

While the central macular lesion exhibited the most severe alterations, significant atrophic changes were also observed throughout the peripheral retina, indicating the retina-wide nature of this degeneration. The ONL thinning and RPE discontinuity demonstrated a severity gradient, most prominent centrally and gradually diminishing towards the periphery, yet remaining evident across the entire retina.

These OCT findings corroborate and extend the observations from fundus photography and fluorescein angiography, providing a detailed cross-sectional view of the retinal structural changes. The absence of membranes or pigment deposits, coupled with the prominent RPE and outer retinal atrophy, further characterizes the distinct nature of this retinal degeneration.

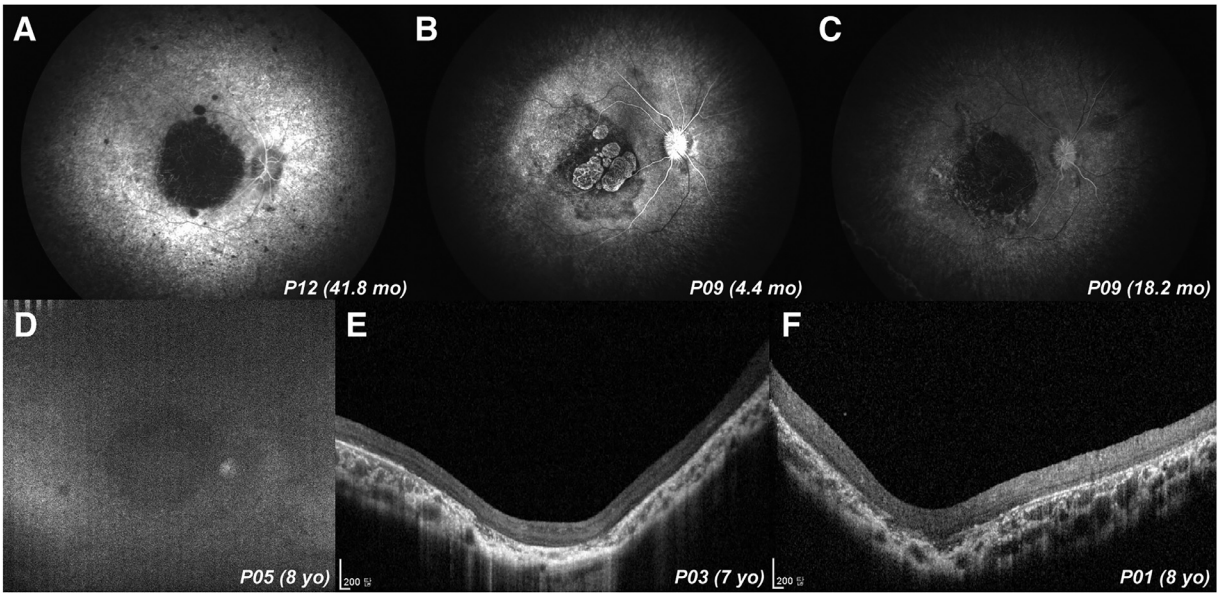

FIGURE 2. Multimodal imaging findings of patients with *NMNAT1* variants. A, FA shows well-demarcated central hypofluorescence with surrounding hypofluorescent patches. B, FA of Patient 9 at 4.4 months demonstrates hyperfluorescent patches within the hypofluorescent region. C, FA of Patient 9 at 18.2 months exhibits similar features as observed in other patients. D, FAF image of a patient shows areas of hypofluorescence. E, F, OCT images demonstrate significant retinal thinning and loss of retinal architecture.

• **VISUAL ACUITY:** Patients with the *NMNAT1* c.709C>T variant demonstrated severe visual impairment, correlating with significant structural abnormalities observed on retinal imaging ($n = 14$, follow-up range: 43.2–136.4 months). The majority of patients ($n = 12$) retained light perception (LP) vision or better in the best-seeing eye. Notably, early fixation and following (F&F) behavior, observed before 1 year of age, was associated with preservation of hand motion (HM) vision or better. In contrast, those unable to perform F&F during infancy typically retained only LP vision.

Patients harboring the c.196C>T variant on the second allele maintained LP vision without demonstrable F&F behavior during infancy. In contrast, patients with the c.116-2A>G variant on the second allele exhibited F&F behavior in infancy, coinciding with the period before complete macular scar formation. Patients 6 and 8 (c.116-2A>G variant), and Patient 12 (exon 2 deletion) retained HM vision or better during long-term follow-up period. Notably, Patients 13 and 14, who did not harbor the c.709C>T variant, exhibited relatively preserved VA, maintaining the ability to perform finger counting. Longitudinal analysis of VA revealed no significant measurable deterioration after 2 years of age in most patients ($n = 12$). In 2 cases, unilateral progression from LP to no light perception (NLP) was documented after follow-up periods of 24 months and 12 months, respectively, underscoring the potential for ongoing degeneration despite apparent VA stability.

• **OTHER CLINICAL FINDINGS AND OPHTHALMOLOGICAL CHARACTERISTICS:** ERG and VEP demonstrated markedly reduced amplitudes with non-specific waveforms in all patients who underwent these assessments ($n = 10$ and $n = 8$, respectively; Figure 3). From infancy, these electrophysiological tests consistently revealed either absent responses or unidentifiable peaks, indicating severe retinal dysfunction and compromised visual pathway integrity. GVF assessment was not feasible for all patients due to severe vision impairment. Refractive examinations revealed hyperopia in all patients, ranging from +1.00 to +9.50 diopters. Most patients exhibited oculodigital signs ($n = 7$), cataracts ($n = 9$), and vitreous opacities on USG ($n = 8$). Nystagmus was consistently observed in all patients with available medical records ($n = 12$). Three patients had developmental delays potentially secondary to visual impairment; however, most patients did not experience any systemic symptoms. One patient (Patient 1) developed exudative retinal detachment accompanied by telangiectasia, suggestive of Coats-like exudative vitreoretinopathy.[28] This condition, known to occur in some inherited retinal disorders, necessitated surgical intervention. The patient subsequently underwent external drainage of the subretinal fluid to manage this complication. The procedure resulted in the removal of 1.5 cc of fluid, leading to significant flattening of the retina and a decrease in subretinal fluid.

DISCUSSION

This study presents a comprehensive analysis of the clinical phenotypes in 14 patients with LCA harboring biallelic

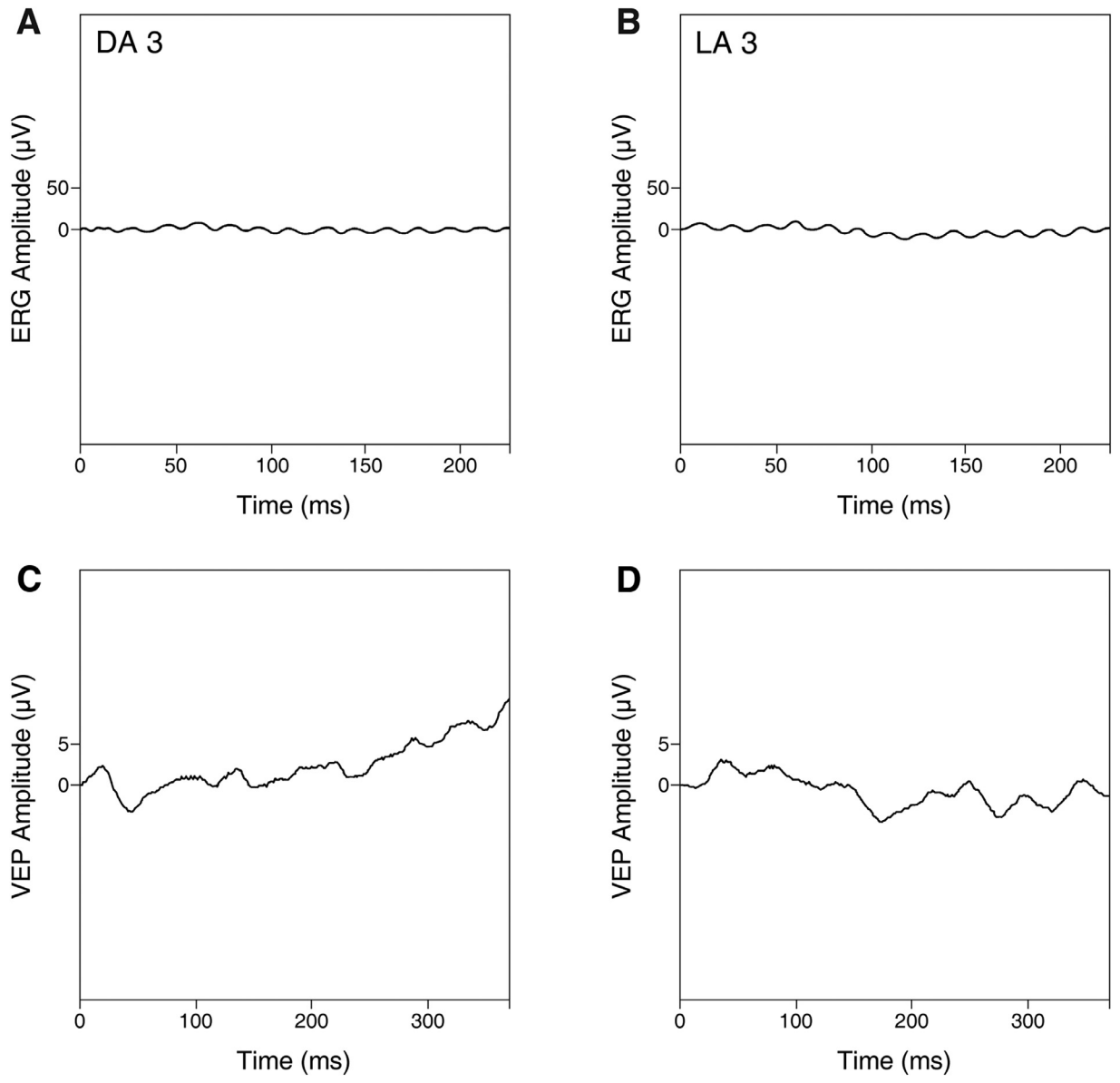

FIGURE 3. Representative electrophysiological findings. A, B, Full-field ERG demonstrates the absence of detectable signals in Patient 13 at 4 years of age: scotopic (DA 3) (A) and photopic (LA 3) (B) responses. C, D, VEP exhibits no discernible peaks and non-specific patterns in both eyes of Patient 3 at 4.7 months of age: OD (C) and OS (D). ERG = electroretinography; VEP = visual-evoked potential; DA = dark-adapted; LA = light-adapted.

NMNAT1 variants. The findings contribute to the current understanding of *NMNAT1*-associated LCA and offer additional insights into the clinical course and potential prognosis of this inherited retinal disorder.

The *NMNAT1* c.709C>T variant is most prevalent in East Asian and Australian populations, while the c.769G>A (p.Glu257Lys) variant is more common in Caucasian populations.[8] Notably, the minor allele frequency (MAF) of *NMNAT1* c.709C>T is significantly higher in the South Korean population (0.001048) compared to the global average (0.00004951) and the East Asian general population (0.0002005).[10,29] The high frequency of this variant in our study population is noteworthy and may suggest a potential founder effect, although further genetic and population studies are required to confirm this hypothesis. The observed prevalence highlights the need for targeted research and intervention strategies specific to this variant.

Our findings of severe, early-onset retinal degeneration align with previous reports on *NMNAT1*-associated LCA.[8,12,16-22] This study enhances the current understanding by providing a more comprehensive temporal and spatial characterization of disease progression. *NMNAT1* variants in patients with LCA are associated with a particularly aggressive form of macular atrophy, resulting in poorer visual outcomes compared to other LCA subtypes.[10] The detailed timeline of disease progression elucidated in this

study offers insights into the development and timing of potential therapeutic interventions.

The NMNAT1 protein plays a crucial role in NAD+ biosynthesis, a crucial cellular metabolite involved in energy production and cellular stress responses.[14,19,20] While some studies have explored the potential relationship between NMNAT1 function and retinal degeneration, the exact mechanisms remain unclear. An in vivo study using *Nmnat1*$^{E257K/-}$ mice reported retinal degeneration and exacerbated photoreceptor damage when exposed to light.[15] Similarly, in *Drosophila* models, light exposure was associated with photoreceptor cell death, while *nmnat* overexpression provided protective effects against light-induced neuronal degeneration.[30] These observations suggest a complex interplay between NMNAT1 function, retinal development, and potential environmental factors such as light exposure. The pattern of central retinal degeneration observed in *NMNAT1*-associated LCA patients is intriguing, but its relationship to focused light exposure or other factors requires further investigation.[16]

The progression of retinal degeneration in *NMNAT1*-associated conditions likely involves multiple factors, including genetic, developmental, and possibly environmental influences. The apparent changes in disease progression rate over time may be due to various factors, such as the natural history of the disease, potential compensatory mechanisms, or limitations in our current assessment methods. It is crucial to consider that the retina may never have developed normally in these patients, complicating the interpretation of postnatal influences on disease progression.

Further research is needed to elucidate the complex pathophysiology of *NMNAT1*-associated LCA. This could include studies on NAD+ levels in different retinal regions, detailed analysis of retinal development in animal models, and longitudinal studies in human patients from early infancy. Such comprehensive approaches may provide valuable insights into the disease mechanisms and potentially inform future therapeutic strategies.

NMNAT1-associated LCA exhibits distinct features compared to other LCA genotypes, underscoring the genetic heterogeneity of this condition. *RPE65*-LCA often presents with relatively preserved retinal structure, which has made it a prime target for therapeutic interventions.[31,32] In contrast, *NMNAT1*-LCA is characterized by rapid and severe retinal degeneration, presenting challenges for potential treatments. *GUCY2D*-LCA demonstrates a different phenotypic profile, with relatively preserved outer retinal structure on OCT and normal fundus appearance, coupled with a greater degree of day-blindness than night-blindness.[31,33] VA in *GUCY2D*-LCA is similarly poor to *NMNAT1*-LCA, with most patients having vision worse than HM, and tends to remain stable over time.[33,34] Patients with *AIPL1*-LCA are characterized by severely reduced VA (although often better than LP), pigmentary changes, and macular atrophy.[35,36] Notably, both *AIPL1*-LCA and *NMNAT1*-LCA patients typically lack residual outer retinal structure by 4 years of age, potentially limiting the therapeutic window.[31] These genotype-specific differences underscore the importance of precise genetic diagnosis in LCA, informing prognosis, guiding management, and directing potential therapeutic approaches, thus highlighting the evolving landscape of LCA from a uniform diagnosis to a spectrum of genetically distinct entities with varying natural histories.

In our study, FA revealed central hypofluorescence, likely due to diminished blood flow resulting from progressive retinal degeneration and atrophy, along with vascular loss. In 1 patient (Patient 9) with early FA images, findings correlated with early fundus changes, revealing hyperfluorescent patches that matched the atrophic patches observed in fundus photography. These patches were reminiscent of window defects showing choroidal vessels, which may indicate RPE defects. Initially, these patches demonstrated hyperfluorescence but later transitioned to hypofluorescence, as observed in other patients. This transition could suggest progressive changes in retinal and/or RPE structure and function. Additionally, FA revealed hypofluorescent areas that were not readily apparent in fundus photographs, indicating functional alterations preceding anatomical changes. Diminished FAF signals were consistent with RPE changes, though the primary cause of these changes remains to be determined.

OCT analysis revealed significant structural changes in the retinas of patients harboring *NMNAT1* variants. These findings support the view that the hypofluorescence of colobomatous lesions observed on FA results from tissue atrophy rather than fluorescence blockage.

The observed maintenance of VA in most patients after 2 years of age presents a critical consideration for potential therapeutic interventions in *NMNAT1*-associated LCA. This suggests a potential therapeutic window during early childhood, before the disease reaches a relatively stable phase. However, it is crucial to interpret this stability cautiously, as it may not necessarily indicate a cessation of underlying retinal degeneration. The identification of this potential therapeutic window has significant implications for both clinical management and research directions. It may inform the optimal timing for gene-based therapies, which could be most effective if administered before irreversible structural changes occur. Additionally, this information could guide the development of cell-based therapies, which might be viable options even after the initial rapid progression phase. These insights can help shape the design of future clinical trials, potentially maximizing therapeutic efficacy and guiding personalized patient counseling regarding prognosis and treatment options.

While there are currently no approved gene-specific treatments for *NMNAT1*-associated LCA, ongoing research is exploring potential therapeutic strategies. Current management primarily focuses on supportive care, encompassing low vision aids, refractive correction, lifestyle modifications (such as smoking cessation and UV protection),

and specialized education.[37] Additionally, treatment of associated complications, including cataracts and vitreoretinal abnormalities, forms an integral part of patient care. Potential therapeutic interventions for *NMNAT1*-associated LCA are being explored, with a focus on gene therapy approaches. Several preclinical studies have demonstrated the potential of adeno-associated virus (AAV)-mediated gene therapy in animal models of *NMNAT1*-associated retinal degeneration.[13,38] Furthermore, pharmacologic and genetic therapies aimed at restoring cellular NAD+ homeostasis in retinal cells may offer promising therapeutic strategies for *NMNAT1*-associated LCA.[12]

While our study focused on *NMNAT1*-associated LCA, it is important to note that *NMNAT1* variants have been implicated in a broader spectrum of disorders. In addition to LCA, *NMNAT1* variants can be associated with a range of phenotypes, including spondyloepiphyseal dysplasia, sensorineural hearing loss, and intellectual disability.[39,40] Moreover, a recent study has proposed a potential link between *NMNAT1* variants and hereditary spastic paraplegia, further expanding the phenotypic spectrum.[41] This finding suggests that *NMNAT1* may play a role in neurological functions beyond the retina, highlighting the need for a more comprehensive understanding of its physiological roles in various tissues.

The limitations of our study include its retrospective design and relatively small sample size, which precluded definitive statistical analyses of genotype-phenotype correlations. Although we addressed the second allele in our analysis, the compound heterozygous nature of the *NMNAT1* variants in our cohort necessitates further investigation into the potential influence of the second allele on the observed phenotypes, which may contribute to the variability in clinical presentations. Additionally, the single-center design may have limited the generalizability of our findings to other populations. Further multi-center studies with larger patient cohorts are warranted to validate the observed genotype-phenotype correlations and explore potential variations within the clinical spectrum of *NMNAT1*-associated retinal dystrophy.

In conclusion, our study highlights the distinct clinical features and potential genotype-phenotype correlations in *NMNAT1*-associated LCA, focusing on the c.709C>T variant. These findings enhance our understanding of the disease progression, which is crucial for patient management and counseling. Future studies should involve functional analyses using patient-derived induced pluripotent stem cells to provide valuable insights into the cellular mechanisms underlying the *NMNAT1*-mediated retinal degeneration. As gene therapy continues to show promise in other forms of LCA, our findings underscore the potential of similar approaches for *NMNAT1*-associated LCA, particularly in populations with a high prevalence of the c.709C>T variant.

CREDIT AUTHORSHIP CONTRIBUTION STATEMENT

YOO JIN LEE: Writing – review & editing, Writing – original draft, Visualization, Methodology, Investigation, Data curation, Conceptualization. **HYUN CHUL JEONG:** Methodology, Investigation. **JEONG HUN KIM:** Writing – review & editing, Investigation, Funding acquisition. **DONG HYUN JO:** Writing – original draft, Investigation, Funding acquisition, Conceptualization.

Funding/Support: Genome editing research program funded by the Korea government (MSIT) (RS-2023-00260351) (Jo), National Research Foundation of Korea (NRF) grant funded by the Korean government (MSIT) (2022R1A2C1003768) (Jo), the Kun-hee Lee Child Cancer and Rare Disease Project (202200004004) (Kim), Seoul National University Hospital Research Grant (18-2023-0010) (Kim), National Research Council of Science & Technology (NST) grant by the Korea government (MSIT) (GTL24021-500) (Kim). Financial Disclosures: No financial disclosures. Declaration of competing interest: The authors declare that they have no known competing financial interests or personal relationships that could have appeared to influence the work reported in this paper.
Acknowledgments: None.

REFERENCES

1. Tsang SH, Sharma T. Leber congenital amaurosis. *Adv Exp Med Biol*. 2018;1085:131–137. doi:10.1007/978-3-319-95046-4_26.
2. Koenekoop RK. An overview of Leber congenital amaurosis: a model to understand human retinal development. *Surv Ophthalmol*. 2004;49(4):379–398. doi:10.1016/j.survophthal.2004.04.003.
3. Stone EM. Leber congenital amaurosis - a model for efficient genetic testing of heterogeneous disorders: LXIV Edward Jackson Memorial Lecture. *Am J Ophthalmol*.. 2007;144(6):791–811 Dec. doi:10.1016/j.ajo.2007.08.022.
4. Chacon-Camacho OF, Zenteno JC. Review and update on the molecular basis of Leber congenital amaurosis. *World J Clin Cases*. 2015;3(2):112–124. doi:10.12998/wjcc.v3.i2.112.
5. den Hollander AI, Roepman R, Koenekoop RK, Cremers FP. Leber congenital amaurosis: genes, proteins and disease mechanisms. *Prog Retin Eye Res*. 2008;27(4):391–419. doi:10.1016/j.preteyeres.2008.05.003.
6. Coussa RG, Lopez Solache I, Koenekoop RK. Leber congenital amaurosis, from darkness to light: an ode to Irene Maumenee. *Ophthalmic Genet*. 2017;38(1):7–15. doi:10.1080/13816810.2016.1275021.
7. Huang CH, Yang CM, Yang CH, Hou YC, Chen TC. Leber's congenital amaurosis: current concepts of genotype-

phenotype correlations. *Genes (Basel)*. 2021;12(8):1261. doi:10.3390/genes12081261.
8. Yi Z, Li S, Wang S, Xiao X, Sun W, Zhang Q. Clinical features and genetic spectrum of NMNAT1-associated retinal degeneration. *Eye (Lond)*. 2022;36(12):2279–2285. doi:10.1038/s41433-021-01853-y.
9. Thompson JA, De Roach JN, McLaren TL, et al. The genetic profile of Leber congenital amaurosis in an Australian cohort. *Mol Genet Genomic Med*. 2017;5(6):652–667. doi:10.1002/mgg3.321.
10. Surl D, Shin S, Lee ST, et al. Copy number variations and multiallelic variants in Korean patients with Leber congenital amaurosis. *Mol Vis*.. 2020;26:26–35.
11. Hosono K, Nishina S, Yokoi T, et al. Molecular diagnosis of 34 Japanese families with leber congenital amaurosis using targeted next generation sequencing. *Sci Rep*. 2018;8(1):8279. doi:10.1038/s41598-018-26524-z.
12. Falk MJ, Zhang Q, Nakamaru-Ogiso E, et al. NMNAT1 mutations cause Leber congenital amaurosis. *Nat Genet*. 2012;44(9):1040–1045. doi:10.1038/ng.2361.
13. Brown EE, Scandura MJ, Pierce EA. Expression of NMNAT1 in the photoreceptors is sufficient to prevent NMNAT1-associated retinal degeneration. *Mol Ther Methods Clin Dev*. 2023;29:319–328. doi:10.1016/j.omtm.2023.04.003.
14. Zhou T, Kurnasov O, Tomchick DR, et al. Structure of human nicotinamide/nicotinic acid mononucleotide adenylyltransferase. Basis for the dual substrate specificity and activation of the oncolytic agent tiazofurin. *J Biol Chem*. 2002;277(15):13148–13154. doi:10.1074/jbc.M111469200.
15. Eblimit A, Zaneveld SA, Liu W, et al. NMNAT1 E257K variant, associated with Leber Congenital Amaurosis (LCA9), causes a mild retinal degeneration phenotype. *Exp Eye Res*. 2018;173:32–43. doi:10.1016/j.exer.2018.04.010.
16. Perrault I, Hanein S, Zanlonghi X, et al. Mutations in NMNAT1 cause Leber congenital amaurosis with early-onset severe macular and optic atrophy. *Nat Genet*. 2012;44(9):975–977. doi:10.1038/ng.2357.
17. Chiang PW, Wang J, Chen Y, et al. Exome sequencing identifies NMNAT1 mutations as a cause of Leber congenital amaurosis. *Nat Genet*. 2012;44(9):972–974. doi:10.1038/ng.2370.
18. Koenekoop RK, Wang H, Majewski J, et al. Mutations in NMNAT1 cause Leber congenital amaurosis and identify a new disease pathway for retinal degeneration. *Nat Genet*. 2012;44(9):1035–1039. doi:10.1038/ng.2356.
19. Kayazawa T, Kuniyoshi K, Hatsukawa Y, et al. Clinical course of a Japanese girl with Leber congenital amaurosis associated with a novel nonsense pathogenic variant in NMNAT1: a case report and mini review. *Ophthalmic Genet*. 2022;43(3):400–408. doi:10.1080/13816810.2021.2023195.
20. Deng Y, Huang H, Wang Y, et al. A novel missense NMNAT1 mutation identified in a consanguineous family with Leber congenital amaurosis by targeted next generation sequencing. *Gene*. 2015;569(1):104–108. doi:10.1016/j.gene.2015.05.038.
21. Hedergott A, Volk AE, Herkenrath P, et al. Clinical and genetic findings in a family with NMNAT1-associated Leber congenital amaurosis: case report and review of the literature. *Graefes Arch Clin Exp Ophthalmol*. 2015;253(12):2239–2246. doi:10.1007/s00417-015-3174-0.
22. Siemiatkowska AM, van den Born LI, van Genderen MM, et al. Novel compound heterozygous NMNAT1 variants associated with Leber congenital amaurosis. *Mol Vis*.. 2014;20:753–759.
23. Bedoukian EC, Zhu X, Serrano LW, Scoles D, Aleman TS. NMNAT1-associated cone-rod dystrophy: evidence for a spectrum of foveal maldevelopment. *Retin Cases Brief Rep*. 2022;16(3):385–392. doi:10.1097/icb.0000000000000992.
24. Jacobson SG, Cideciyan AV, Ratnakaram R, et al. Gene therapy for leber congenital amaurosis caused by RPE65 mutations: safety and efficacy in 15 children and adults followed up to 3 years. *Arch Ophthalmol*. 2012;130(1):9–24. doi:10.1001/archophthalmol.2011.298.
25. Robson AG, Frishman LJ, Grigg J, et al. ISCEV Standard for full-field clinical electroretinography (2022 update). *Doc Ophthalmol*. 2022;144(3):165–177. doi:10.1007/s10633-022-09872-0.
26. Odom JV, Bach M, Brigell M, et al. ISCEV standard for clinical visual evoked potentials: (2016 update). *Doc Ophthalmol*. 2016;133(1):1–9. doi:10.1007/s10633-016-9553-y.
27. Richards S, Aziz N, Bale S, et al. Standards and guidelines for the interpretation of sequence variants: a joint consensus recommendation of the American College of Medical Genetics and Genomics and the Association for Molecular Pathology. *Genet Med*. 2015;17(5):405–424. doi:10.1038/gim.2015.30.
28. Han J, Kim TY, Kim M. Coats-like Exudative Vitreoretinopathy in NMNAT1 Leber Congenital Amaurosis. *Ophthalmol Retina*. 2021;5(7):624. doi:10.1016/j.oret.2021.04.010.
29. Karczewski KJ, Francioli LC, Tiao G, et al. The mutational constraint spectrum quantified from variation in 141,456 humans. *Nature*. 2020;581(7809):434–443. doi:10.1038/s41586-020-2308-7.
30. Zhai RG, Cao Y, Hiesinger PR, et al. Drosophila NMNAT maintains neural integrity independent of its NAD synthesis activity. *PLoS Biol*. 2006;4(12):e416. doi:10.1371/journal.pbio.0040416.
31. Georgiou M, Robson AG, Fujinami K, et al. Phenotyping and genotyping inherited retinal diseases: molecular genetics, clinical and imaging features, and therapeutics of macular dystrophies, cone and cone-rod dystrophies, rod-cone dystrophies, Leber congenital amaurosis, and cone dysfunction syndromes. *Prog Retin Eye Res*. 2024;100:101244. doi:10.1016/j.preteyeres.2024.101244.
32. Kumaran N, Georgiou M, Bainbridge JWB, et al. Retinal Structure in RPE65-Associated Retinal Dystrophy. *Invest Ophthalmol Vis Sci*. 2020;61(4):47. doi:10.1167/iovs.61.4.47.
33. Bouzia Z, Georgiou M, Hull S, et al. GUCY2D-Associated Leber Congenital Amaurosis: a Retrospective Natural History Study in Preparation for Trials of Novel Therapies. *Am J Ophthalmol*. 2020;210:59–70. doi:10.1016/j.ajo.2019.10.019.
34. Hahn LC, Georgiou M, Almushattat H, et al. The natural history of leber congenital amaurosis and cone-rod dystrophy associated with variants in the GUCY2D Gene. *Ophthalmol Retina*. 2022;6(8):711–722. doi:10.1016/j.oret.2022.03.008.
35. Sacristan-Reviriego A, Le HM, Georgiou M, et al. Clinical and functional analyses of AIPL1 variants reveal mechanisms of pathogenicity linked to different forms of retinal degeneration. *Sci Rep*. 2020;10(1):17520. doi:10.1038/s41598-020-74516-9.
36. Zhang Q, Sun J, Liu Z, et al. Clinical and Molecular Characterization of AIPL1-Associated Leber Congenital

Amaurosis/Early-Onset Severe Retinal Dystrophy. *Am J Ophthalmol*. 2024;266:235–247. doi:10.1016/j.ajo.2024.06.013.
37. Daich Varela M, Cabral de Guimaraes TA, Georgiou M, Michaelides M. Leber congenital amaurosis/early-onset severe retinal dystrophy: current management and clinical trials. *Br J Ophthalmol*. 2022;106(4):445–451. doi:10.1136/bjophthalmol-2020-318483.
38. Greenwald SH, Brown EE, Scandura MJ, et al. Gene Therapy Preserves Retinal Structure and Function in a Mouse Model of NMNAT1-Associated Retinal Degeneration. *Mol Ther Methods Clin Dev*. 2020;18:582–594. doi:10.1016/j.omtm.2020.07.003.
39. Bedoni N, Quinodoz M, Pinelli M, et al. An Alu-mediated duplication in NMNAT1, involved in NAD biosynthesis, causes a novel syndrome, SHILCA, affecting multiple tissues and organs. *Hum Mol Genet*. 2020;29(13):2250–2260. doi:10.1093/hmg/ddaa112.
40. Abad-Morales V, Wert A, Ruiz Gómez M, Navarro R, Pomares E. New Insights on the Genetic Basis Underlying SHILCA Syndrome: characterization of the NMNAT1 Pathological Alterations Due to Compound Heterozygous Mutations and Identification of a Novel Alternative Isoform. *Int J Mol Sci*. 2021;22(5):2262. doi:10.3390/ijms22052262.
41. Sadr Z, Ghasemi A, Rohani M, Alavi A. NMNAT1 and hereditary spastic paraplegia (HSP): expanding the phenotypic spectrum of NMNAT1 variants. *Neuromuscul Disord*. 2023;33(4):295–301. doi:10.1016/j.nmd.2023.02.001.